INTERNATIONAL JOURNAL of PARTICLE THERAPY

A Probability-Based Investigation on the Setup Robustness of Pencil-beam Proton Radiation Therapy for Skull-Base Meningioma

Wei Zou, PhD; Goldie Kurtz, MD; Mayisha Nakib, PhD; Brendan Burgdorf, MS; Murat Alp, PhD; Taoran Li, PhD; Robert Lustig, MD; Ying Xiao, PhD; Lei Dong, PhD; Alireza Kassaee, PhD; Michelle Alonso-Basanta, MD

Department of Radiation Oncology, Hospital of the University of Pennsylvania, Philadelphia, PA, USA

Abstract

Introduction: The intracranial skull-base meningioma is in proximity to multiple critical organs and heterogeneous tissues. Steep dose gradients often result from avoiding critical organs in proton treatment plans. Dose uncertainties arising from setup errors under image-guided radiation therapy are worthy of evaluation.

Patients and Methods: Fourteen patients with skull-base meningioma were retrospectively identified and planned with proton pencil beam scanning (PBS) single-field uniform dose (SFUD) and multifield optimization (MFO) techniques. The setup uncertainties were assigned a probability model on the basis of prior published data. The impact on the dose distribution from nominal 1-mm and large, less probable setup errors, as well as the cumulative effect, was analyzed. The robustness of SFUD and MFO planning techniques in these scenarios was discussed.

Results: The target coverage was reduced and the plan dose hot spot increased by all setup uncertainty scenarios regardless of the planning techniques. For 1 mm nominal shifts, the deviations in clinical target volume (CTV) coverage D99% was -11 ± 52 cGy and -45 ± 147 cGy for SFUD and MFO plans. The setup uncertainties affected the organ at risk (OAR) dose both positively and negatively. The statistical average of the setup uncertainties had <100 cGy impact on the plan qualities for all patients. The cumulative deviations in CTV D95% were 1 ± 34 cGy and -7 ± 18 cGy for SFUD and MFO plans.

Conclusion: It is important to understand the impact of setup uncertainties on skull-base meningioma, as the tumor target has complex shape and is in proximity to multiple critical organs. Our work evaluated the setup uncertainty based on its probability distribution and evaluated the dosimetric consequences. In general, the SFUD plans demonstrated more robustness than the MFO plans in target coverages and brainstem dose. The probability-weighted overall effect on the dose distribution is small compared to the dosimetric shift during single fraction.

Keywords: BOS meningioma; setup robustness; PBS proton radiation therapy

Submitted 25 Feb 2020
Accepted 19 Oct 2020
Published 28 Jan 2021

Corresponding Author:
Wei Zou, PhD
Department of Radiation Oncology
University of Pennsylvania
Philadelphia, PA 19104, USA
Phone: +1 (800) 789-7366
Wei.Zou@pennmedicine.upenn.edu

Original Article

DOI
10.14338/IJPT-20-00009.1

http://theijpt.org

Introduction

Meningiomas are tumors arising from the meninges, the thin layers of tissue surrounding the brain and spinal cord. These tumors, typically benign, account for approximately 36% of all primary brain tumors [1]. While complete surgical resection is considered the optimal treatment for this diagnosis, tumors are often deemed unresectable owing to their anatomic locations. Radiation therapy provides an alternative treatment of unresectable meningioma that can direct radiation beams toward the tumor while attempting to spare adjacent critical structures such as the brainstem, optic nerves, and optic chiasm [2–5]. Patients with meningioma have been historically treated with external photon beam radiation therapy [5–9] or stereotactic radiosurgery [10, 11]. A previous study showed the advantage of intensity-modulated photon radiation therapy (IMRT) over conformal radiation therapy by a 36% increase in target coverage and a 10% increase in dose conformality [6]. Other studies showed the safety of IMRT for treating meningioma at the skull base [7–9]. Proton beams deliver different depth-dose curves than photon beams where no dose is delivered beyond Bragg peak. Proton therapy could offer advantages over photon therapy to spare healthy organs at risk (OARs) for patients with meningioma. Vernimmen et al [12] have used protons for stereotactic and hypofractionated stereotactic proton radiation therapy for skull-base meningioma and obtained $>$88% radiologic control. Efficacy and safety using passive scattering proton radiation therapy were demonstrated [13–15]. Proton pencil beam and dose painting methods were also used for effective treatment of meningioma [16–18], where general dose reduction to brain, brainstem, and optic apparatus, as compared to IMRT plans, was observed.

Skull-base meningioma tumors can grow to considerable sizes and often have complex shapes. In skull-base meningioma proton radiation therapy, the proton beams inevitably penetrate through heterogeneous intracranial structures before arriving at the tumor target. The proton beams can be arranged to provide adequate coverage to the complexly shaped tumor with a sharp dose gradient at the tumor boundary to avoid dose to the brainstem, optic nerves, optic chiasm, and cochlea that are in proximity. As proton dose distribution is susceptible to the heterogeneity along the beam path, the impact of setup uncertainties is of interest. In the setup of intracranial patients, orthogonal kV and cone-beam computed tomography (CT) are used as image guidance to position the patients under mask [19–21] and result in a distribution of setup uncertainties. Our current clinical treatment planning system Eclipse (Varian, Palo Alto, California) offers a robust optimization module that optimizes the spot intensities to provide sufficient target coverage under the worst setup and range uncertainty scenarios. However, the effects of the probability in the setup uncertainties cannot be considered in the plan optimization process or during the final dose evaluation. The clinical plan qualities are evaluated on each of the setup and range uncertainty scenarios. In these complex meningioma cases, the plan dosimetric constraints cannot be met for all the worst setup scenarios. This study provides dose analysis from a novel bimodal Gaussian setup uncertainty distribution model where setup in the positive and negative directions are considered to be equally possible. The consequent dosimetric effects in the tumor target coverage and critical organ avoidance, due to various setup uncertainty values, were considered. The statistical summation of the dose effects from the setup distribution was obtained. This approach was applied to both single-field uniform dose (SFUD) and multifield optimization (MFO) proton pencil beam scanning (PBS) plans for patients with skull-base meningioma, and their sensitivity to the setup uncertainties was analyzed.

Materials and Methods

After approval by the Institutional Review Board, patient selection was determined by using ICD-9 and ICD-10 codes as well as intracranial location. Fourteen patients who had undergone radiation at our facility were identified with meningioma tumors located at the base of skull. Physician-defined planning treatment volume (PTV) expands the clinical target volume (CTV) using a 5-mm margin, which can be reduced based on its extension into the OARs and the extensiveness of the patient-specific disease. The PTVs of this adult patient cohort have a mean of 137.2 cm^3 and a standard deviation of 117.7 cm^3. The tumor locations and their volumes are listed in **Table 1**. We used the Eclipse treatment planning system to construct base plans with proton PBS techniques with a prescription of relative biological effectiveness (RBE) dose 5400 cGy in 30 fractions. RBE is set to 1.1 in Eclipse. All dose values in this article refer to the RBE dose. For each patient, one plan was generated with the SFUD technique, and another plan was generated with the MFO technique.

The patients underwent CT scanning at 1.5-mm slice thickness on a Siemens SOMATOM CT scanner (Siemens Medical Solutions USA, Malvern, Pennsylvania), immobilized with thermoplastic masks. A U-shaped bolus with 6.2-cm water equivalent thickness was used around the patient's head to increase the plan minimum energy to be above the minimum machine deliverable energy of 100 MeV. The beam angles were chosen by experienced proton dosimetrists to avoid unnecessary brain tissue and critical organs along the beam paths. They were finalized by trial-and-error process for the best

Table 1. Patients in study.

Patient	Location	PTV volume, cm^3
1	Right retro-orbital	136
2	Right cavernous sinus	102.4
3	Left sphenoid	75.5
4	Central frontal sinus	110.9
5	Central base of skull	115.9
6	Right cavernous sinus	51
7	Right retro-orbital/cavernous sinus	157.7
8	Sella turcica	72.9
9	Right sphenoid	150.4
10	Left upper cervical	278
11	Right/central base of skull	32.9
12	Left retro-orbital/cavernous sinus	487.4
13	Right retro-orbital/cavernous sinus	92.5
14	Left retro-orbital/cavernous sinus	56.8

Abbreviation: PTV, planning treatment volume.

achievable dose distributions where the dose to the targets and OARs could satisfy the dosimetric constraints. The dose deviations from the constraints and final plan dose distributions were approved by a radiation oncologist. All but 1 of the cases were planned with 3 proton beams. The remaining case was planned with 2 beams, as the tumor had a small volume and was close to the body surface. The CTVs were expanded to the dosimetric PBS target volumes with 5-mm uniform expansion. The expansion was to take into account the setup uncertainties and the proton range uncertainties. At the region adjacent to critical structures, the PBS target volume is cropped back to 3-mm expansion to avoid the beam spots being populated to them. No robust optimization process was used during the planning process. Our clinic is equipped with both fixed and gantry nozzles. The spots at the fixed nozzle are smaller with sigma varying from 4.5 mm at 100 MeV to 2.6 mm at 200 MeV. The spot sigma in the gantry nozzles varies from 6.5 to 4.0 mm in the same energy range. The patients were planned on the fixed nozzle if no gantry rotations were needed to reduce the impact of the lateral dose spread at tumor boundary due to different spot sizes. The planning optimization goal was to deliver 100% of the prescribed dose to 95% of the PTV volume and limit the hot spot to be $<$110% of the prescription dose. The constraints applied to OARs are detailed in **Table 2**. A radiation oncologist has reviewed these base plans and deemed them clinically acceptable regarding the OAR doses and PTV coverages.

Many articles have reviewed and assessed the setup uncertainties in brain tumors under modern image-guided radiation therapy (IGRT) techniques [22–25]. A typical brain setup is to use kV orthogonal or cone-beam computed tomography (CBCT) to align with the bony anatomy landmarks [22]. Cubillos Mesias et al [23] obtained brain systematic (random) setup errors of 1.0 (1.5), 1.1 (1.4), and 1.0 (1.1) mm in the superior-inferior, left-right, and anterior-posterior directions with CBCT. Tryggestad et al [24] obtained similar values of 1.2 (1.4), 1.1 (1.2), and 1.1 (1.1) mm. Infusino et al [25] measured less than 2.0 mm systematic errors in each direction with a small 0.1- to 0.3-mm random error with kV imaging and 6DoF corrections. With these studies, we adopted the setup uncertainty of 1.0 (1.0) mm for systematic and random error in each direction, where the probability of the setup uncertainties was equal in either superior or inferior, left or right, and anterior or posterior directions. A bimodal Gaussian distribution was constructed to represent the setup uncertainties in this meningioma proton dosimetric

Table 2. Dose constraints for OARs in this study.

Structure	Dose constraints, cGy
Brainstem	D0.03cc $\leq$5400
Optic chiasm	D0.03cc $\leq$5400
Left and right optic nerve	D0.03cc $\leq$5400
Left and right eye	D0.03cc $\leq$4500
Left and right cochlea	D0.03cc $\leq$4500, mean $\leq$3000
Left and right temporal lobe	Mean $\leq$2500

Abbreviation: OARs, organs at risk.

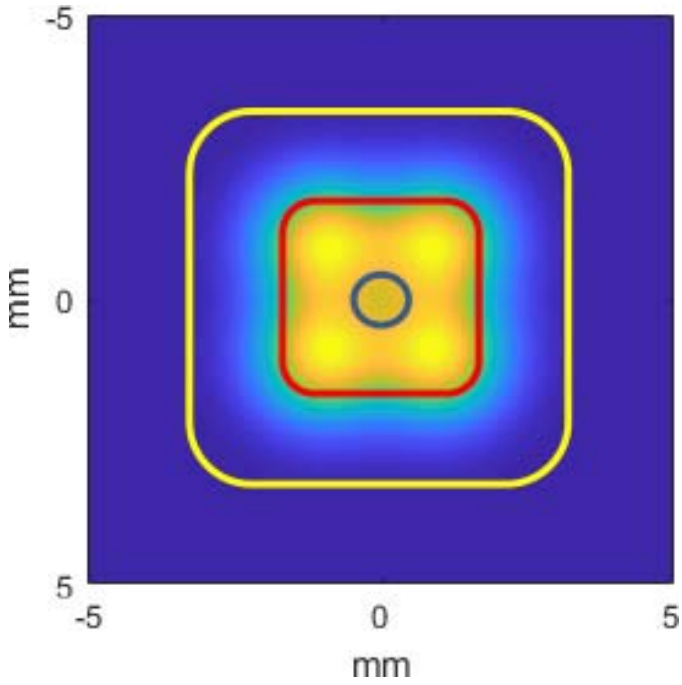

Figure 1. Trivariate bimodal normal distribution illustrated on a 2D plane (after integration of the third axis). The 0, ±1, and ±2.4 mm setup probability bands are bounded by the blue, red, and yellow lines.

study. It is expressed as follows:

$$P(\vec{X}) = \prod_{i=1}^{3} P(X_i) = \prod_{i=1}^{3} \left[\alpha_1 \mathcal{N}_1(X_i | X_{mi}, \sigma_i^2) + \alpha_2 \mathcal{N}_2(X_i | - X_{mi}, \sigma_i^2)\right] \quad (1)$$

Here, the probability of the setup uncertainty in x, y, z directions ($\vec{X}$) is expressed by the weighted trivariate (in x, y, z directions) bimodal normal distributions. $\mathcal{N}_1$ and $\mathcal{N}_2$ are the normal distribution with mean $\pm X_{mi}$ and standard deviation σ_i (i= 1, 2, 3 represents the x, y, and z directions, respectively). The weights $\alpha_1 = \alpha_2 = 0.5$ represent the equal uncertainty probability at the positive/negative directions. Here $\pm X_{mi} = \{\pm 1$ mm, ± 1 mm, ± 1 mm$\}$ and $\sigma_i = \{1$ mm, 1 mm, 1 mm$\}$. An illustrative probability density function of this multimodal setup uncertainty model expressed in the X and Y planes is shown in **Figure 1**. The center band around 0 setup error has lower probability than the band surrounding the mean and the most probable values. The probability of the setup errors larger than the mean value band drops sharply.

When using the Eclipse TPS calculation engine to evaluate the plan dose distribution change due to the setup uncertainties, only a limited number of setup uncertainty values can be input for dose calculation. Therefore, we used Eclipse to analyze a representative dose variation within each setup probability band. For each setup uncertainty band $\vec{X} \in [\overrightarrow{X_a}, \overrightarrow{X_b})$, the cumulative probability (CP) in this setup uncertainty band can be expressed as

$$CP_n = P(\vec{X} \in \left[\overrightarrow{X_a}, \overrightarrow{X_b}\right)) = \iiint_{\overrightarrow{X}_b}^{\overrightarrow{X}_a} \prod_{i=1}^{3} \left[\alpha_1 \mathcal{N}_1(X_i |\ X_{mi}, \sigma_i^2\Big) + \alpha_2 \mathcal{N}_2(X_i | - X_{mi}, \sigma_i^2\Big)\right] dX_1 dX_2 dX_3 \quad (2)$$

Therefore the statistically expected dose from the probable setup can be expressed as

$$\langle D(\vec{X})\rangle = \iiint D(X_1, X_2, X_3) P(X_1, X_2, X_3) dX_1 dX_2 dX_3 \quad (3)$$

and can be approximated by using the probability bands as

$$\langle D(\vec{X})\rangle \approx \sum_{n=1}^{N} D(\rightarrow X_{n0}) * \mathrm{CP}_n \quad (4)$$

$D(\overrightarrow{X_{n0}})$ is a representative dose distribution in the nth of the total N setup bands. When the number of setup bands approaches infinity, Equation 4 becomes Equation 3.

In this study, the center of the setup bands $\overrightarrow{X_{n0}}$ was chosen to be representative of no setup error of 0 mm, mean ±1 mm, and larger ±2.4 mm with the bandwidth of 1 mm, 1.2 mm, and 1.4 mm in each of the x, y, and z directions. The cumulative probability of each band CP_n can be obtained from the 3D cumulative density function. The dose distributions at each of the setup zones were calculated by shifting the isocenter with $\overrightarrow{\pm 1; \text{mm}}$, and $\overrightarrow{\pm 2.4; \text{mm}}$ at X, Y, Z directions from the base plans.

For each patient, the base SFUD and MFO plans were exported from the Eclipse TPS as DICOM-RT plans. A MATLAB software (MathWorks, Natick, Massachusetts) code was developed to read the DICOM-RT file, shift its isocenter in the $\overrightarrow{X_{n0}} = \overrightarrow{0}$, $\overrightarrow{\pm 1; \text{mm}}$, and $\overrightarrow{\pm 2.4; \text{mm}}$ in XYZ directions and generate new plans in DICOM format. The proton beam angles, energies, and spots of the original plans were maintained. A total of 16 SFUD and 16 MFO plans with various isocenter offsets for each patient were generated and imported back into Eclipse. The dose distributions of these plans were recalculated. A Varian Eclipse API script was run to analyze the plan target and OAR dosimetric indexes from **Table 2** to examine the changes due to various setup uncertainties. In addition, taking into account the probability of the setup uncertainties, the statistical cumulative dose distribution was calculated from the base plan and 16 new plans by using the derived band cumulative CP_n and Equation 4.

Results

Across the 14 patients' base plans, the PTV coverage D95% ranged between 5209 and 5376 cGy for SFUD plans, between 5212 and 5397 cGy for MFO plans. The CTV coverage D99% ranged between 4987 and 5416 cGy for SFUD plans, between 4769 and 5392 cGy for MFO plans. The CTV coverage D95% ranged between 5290 and 5445 cGy for SFUD plans, between 5292 and 5435 cGy for MFO plans. The body dose D0.03cc ranged between 5542 and 5800 cGy for SFUD plans, between 5554 and 5854 cGy for MFO plans. Large variations in the dosimetric index among patients were observed for the brainstem, optic chiasm, left and right optic nerve, cochlea, and eyes due to the meningioma target locations and sizes. The min-max ranges of D0.03cc of brainstem among the 14 patients were [1278, 5657] cGy for SFUD plans and [1604, 5595] cGy for MFO plans; D0.03cc of optic nerves were [673, 5428] cGy for SFUD plans and [587, 5396] cGy for MFO plans; D0.03cc of optic chiasm were [3505, 5459] cGy for SFUD plans and [3703, 5408] cGy for MFO plans; D0.03cc of eyes were [∼0, 5064] cGy for SFUD plans and [∼0, 5099] cGy for MFO plan; D0.03cc/mean of the cochlea were [∼0/0, 5507/5475] cGy for SFUD plans and [∼0/0, 5503/5445] cGy for MFO plans. A nonparametric Kruskal-Wallis test was performed to examine dosimetric equivalency between SFUD and MFO plans. Across all the dosimetric indices, the base SFUD and MFO plans did not show significant differences ($P > .49$ for all dosimetric indices).

From the base plans, 1-mm and 2.4-mm setup uncertainties of the 14 patients were applied as described above. The dose distribution due to these setup uncertainties was recalculated in Eclipse TPS. **Figure 2** plots, for patient 14, the dose-volume histogram (DVH) changes from the base plans (solid thick lines) for the 1-mm (fine solid lines) and 2.4-mm (fine dashed lines) setup uncertainties. More extensive spread in DVHs of both CTV coverages and optic chiasm was observed in the MFO plan compared with the SFUD plan.

When the setup uncertainties were introduced, the tumor target coverages were compromised for both SFUD and MFO plans in the entire patient cohort, independent of the direction of the setup error (**Figure 3**). MFO plans in general had more extensive target coverage changes than SFUD plans owing to the setup uncertainties. The changes in the CTV coverage, body max dose, and OAR dosimetric index across the 448 plans of the 14 patients, due to 1-mm or 2.4-mm setup shifts in SFUD or MFO base plans, were calculated. The statistics, including the mean, standard deviation, the 25th, 50th, and 75th percentiles, and range of the changes, of the 112 plans for either 1- or 2.4-mm setup shifts in either SFUD or MFO base plans, are listed in **Table 3**. For a small 1-mm setup error, the mean/max reduction in the CTV D99% coverage was –11/–164 cGy for SFUD and –24/–327 cGy for MFO; the mean/max coverage reduction in CTV D95% was –6/–86 cGy for SFUD and –21/–146 cGy for MFO. The average/max CTV 99% coverage reduction was larger at 2.4-mm setup error with –46/–625 cGy for SFUD and –110/–1040 cGy for MFO. The body hot spot maintained small variations for all SFUD plans and increased for all MFO plans, especially at larger setup errors. The mean and standard deviations for the change in the hot spot for MFO plans under 2.4-mm setup errors were 166 ± 151 cGy.

Figure 4 shows the box plots of the OAR dose changes across the 14 patients from each setup uncertainty scenario. The statistics of the changes from the base plans are listed in **Table 3**. Only patients who had clinically significant doses to the OARs in the base plans, namely, D0.03cc larger than 4500 cGy for the brainstem, optic nerves, and optic chiasm, and larger than 3500 cGy for the eyes and cochleas, were included in the statistical analysis. As expected, larger setup uncertainty caused larger changes in OAR doses. The changes in OAR doses can be either positive or negative, and were sensitive to

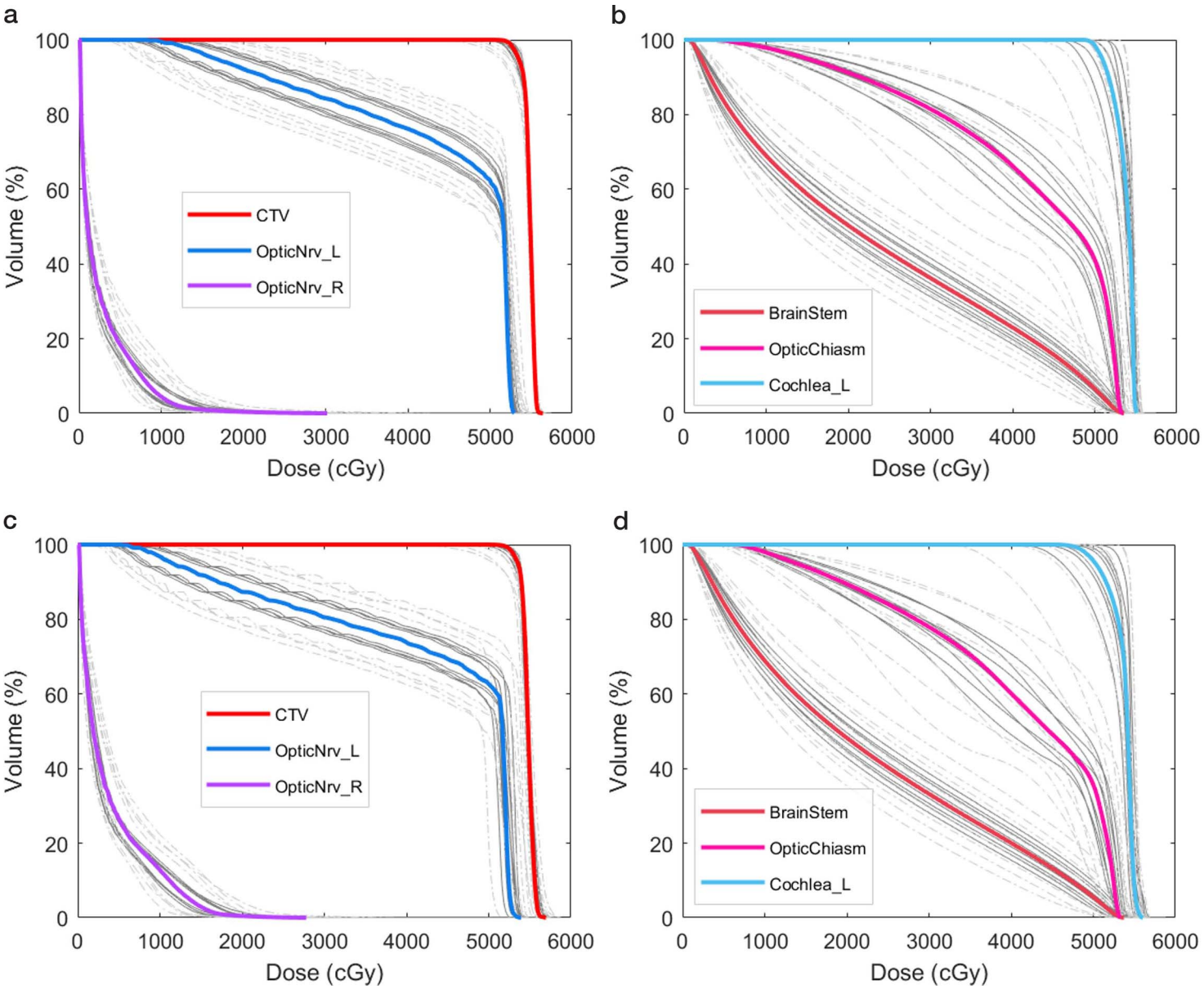

Figure 2. The DVH changes from the base plans (thick colored lines) due to the setup uncertainties for patient 14. (a) and (b) Changes from the SFUD plan. (c) and (d) Changes from the MFO plan for CTV coverage and OARs (solid fine grey lines are from 1-mm setup uncertainties; dashed fine grey lines are from 2.4-mm setup uncertainties). Abbreviations: CTV, clinical target volume; DVH, dose-volume histogram; L, left; MFO, multifield optimization; OARs, organs at risk; OpticNrv, optic nerve; R, right; SFUD, single-field uniform dose.

specific individual setup shift directions. The setup uncertainties affect the dose in cochlea and eyes more significantly than the dose in brainstem, optic nerves, and optic chiasm.

From Equation 4, the overall uncertainty effects are the sum of the weighted plan dose under different setup uncertainty bands. For each patient, the SFUD and MFO plan sums were calculated with the base plan, 8 plans with 1.0-mm setup shifts, and 8 plans with 2.4-mm setup shifts, by using Equation 4. The statistics of the changes in the SFUD and MFO plan sums from the base plans for all the patients were calculated. The mean, standard deviation, the 25th, 50th, and 75th percentiles, and range of the changes in target coverage, body max dose, and OAR dose are shown in **Table 4**. For some patients, CTV still had compromised coverage but to a much lesser extent. The mean and max CTV D99% change was 1/–86 cGy (SFUD) and 7/–30 cGy (MFO). Although for each patient, specific setup uncertainties can have considerable changes in the OAR dose, the statistically averaged total dose change to OARs is smaller than 100 cGy.

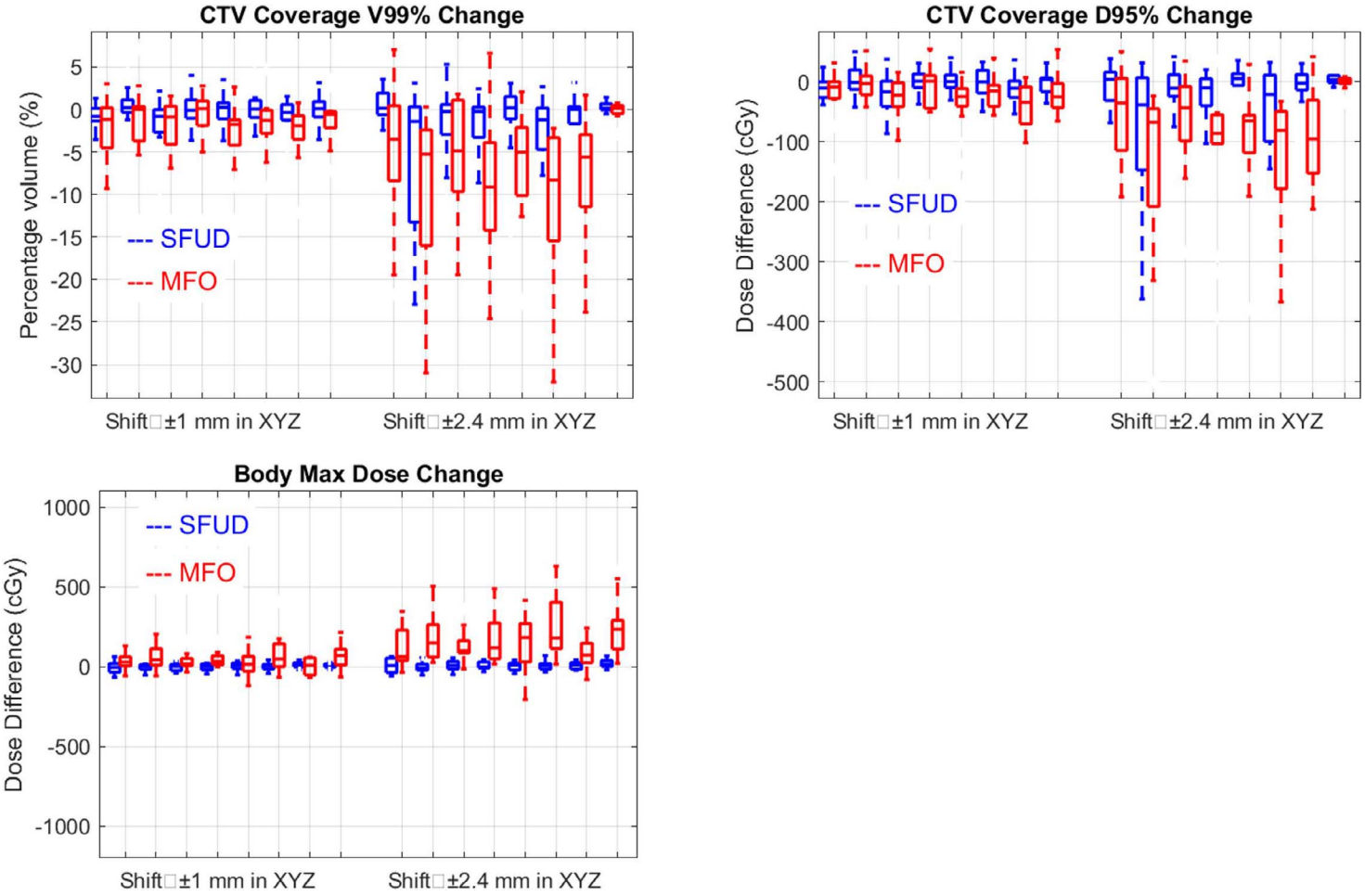

Figure 3. The variations in the CTV coverage D99% and D95% and body max dose for all 14 patients due to ±1 mm and ±2.4 mm shifts in X, Y, Z directions from the SFUD and MFO base plans. Each box plot represents the dosimetric index distribution of the patients at the setup uncertainty scenarios of (1.0, 1.0, 1.0), (–1.0, 1.0, 1.0), (1.0, –1.0, 1.0), (–1.0, –1.0, 1.0), (1.0, 1.0, –1.0), (–1.0, 1.0, –1.0), (1.0, –1.0, –1.0), and (–1.0, –1.0, –1.0) mm; and (2.4, 2.4, 2.4), (–2.4, 2.4, 2.4), (2.4, –2.4, 2.4), (–2.4, –2.4, 2.4), (2.4, 2.4, –2.4), (–2.4, 2.4, –2.4), (2.4, –2.4, –2.4), and (–2.4, –2.4, –2.4) mm (from left to right). Abbreviations: CTV, clinical target volume; MFO, multifield optimization; SFUD, single-field uniform dose.

A nonparametric Kruskal-Wallis test was performed to examine the dosimetric index changes between SFUD and MFO plans due to setup uncertainties. It was found that in SFUD plans, the changes in target coverage CTV D99% and D95% were significantly smaller ($P < .01$ for both) than in MFO plans. Changes in body max dose and brainstem D0.03cc in SFUD plans were also significantly smaller than in MFO plans ($P < .01$ for body max dose, $P = .02$ for brainstem D0.03cc). No significant differences were found for changes in D0.03cc for optic nerves, optic chiasm, eyes, and cochlea between SFUD and MFO plans with $P = .98$, .50, .92 and .11, respectively. No significant dose differences were observed between cumulative SFUD and MFO plans ($P > .20$ for all dosimetric indices).

Discussion

In skull-base meningioma cases, multiple critical organs are in proximity to the tumor. Proton radiation therapy has great advantages in meeting the dose constraints and limiting hot spots in the patient body. This is primarily due to the sharp longitudinal dose fall-off of the proton beam and superior dose-shaping abilities with modulated spot positions and intensities of PBS techniques. The plan spot energies in this study vary from 100.2 to 206.3 MeV with a mean of 172.3 MeV and a standard deviation of 11.9 MeV. In this energy range, the sigma of the pencil beam spot size varies between 2.6 and 6.5 mm as mentioned above. All the SFUD and MFO base plans of these 14 patients met the target and OAR constraints. In these skull-base meningioma cases, the MFO base plans do not show significant advantages over the SFUD plans. The statistical

Table 3. Statistics of the changes in the CTV coverage, body max dose, and OAR dosimetric index for all 14 patients from ±1 or ±2.4 mm setup shifts for SFUD or MFO plans.

Change in	Mean	Std	25%	50%	75%	Min	Max
SFUD: 1-mm shift							
CTV coverage D99%	−11	52	−33	0	22	−164	98
CTV coverage D95%	−6	24	−22	−4	10	−86	50
Body D0.03cc	2	27	−16	5	18	−66	90
Brainstem D0.03cc	7	36	−6	7	21	−177	102
Optic nerve D0.03cc	15	60	−6	14	38	−187	252
Optic chiasm D0.03cc	10	43	−5	13	30	−189	125
Eye D0.03cc	1	178	−134	7	131	−410	387
Cochlea D0.03cc	4	119	−23	12	50	−445	350
SFUD: 2.4-mm shift							
CTV coverage D99%	−45	147	−46	−1	19	−625	178
CTV coverage D95%	−26	71	−39	−2	12	−362	42
Body D0.03cc	9	35	−16	8	30	−58	121
Brainstem D0.03cc	10	96	−16	14	36	−598	241
Optic nerve D0.03cc	20	153	−9	41	97	−529	307
Optic chiasm D0.03cc	18	115	4	49	77	−567	223
Eye D0.03cc	−49	419	−312	−20	293	−1088	755
Cochlea D0.03cc	18	286	−61	24	172	−1059	758
MFO: 1-mm shift							
CTV coverage D99%	−24	87	−72	−17	19	−327	174
CTV coverage D95%	−21	35	−41	−15	−1	−146	55
Body D0.03cc	42	74	4	30	74	−121	406
Brainstem D0.03cc	15	53	−10	18	39	−242	154
Optic nerve D0.03cc	12	82	−39	15	71	−212	215
Optic chiasm D0.03cc	14	46	−17	16	49	−156	124
Eye D0.03cc	1	193	−147	−4	151	−413	370
Cochlea D0.03cc	−6	130	−62	−8	61	−438	373
MFO: 2.4-mm shift							
CTV coverage D99%	−110	231	−180	−62	12	−1040	283
CTV coverage D95%	−88	102	−128	−64	−16	−500	51
Body D0.03cc	166	151	55	123	257	−205	631
Brainstem D0.03cc	48	144	−10	56	111	−737	380
Optic nerve D0.03cc	26	192	−87	56	145	−597	621
Optic chiasm D0.03cc	39	125	−27	50	123	−502	274
Eye D0.03cc	−36	451	−301	−27	360	−1025	724
Cochlea D0.03cc	6	316	−124	13	147	−1041	820

Abbreviations: CTV, clinical target volume; OAR, organ at risk; SFUD, single-field uniform dose; MFO, multifield optimization; Std, standard deviation.

Note: The mean, standard deviation, the 25th, 50th, and 75th percentiles, and range of the changes in the 112 plans (8 plans for each patient) for each scenario are listed. Values are in cGy.

analysis showed that the SFUD plans demonstrated more robust target coverage and brainstem dose than the MFO plans, although both had equivalent setup robustness in dose to optic apparatus and cochlea.

The current TPS provides a robust beam optimization module during the planning process. The optimization process takes a predefined set of values for the setup shifts and range uncertainties and optimizes the beam spots that meet the dose constraints under all the scenarios, regardless of the probabilities of them. A typical setup shift was set to be 3 mm as the "worst scenario." Our study showed that a larger deviation in OAR dose and target coverage exists at larger setup uncertainties. Satisfying the dosimetric constraints under the worst scenarios during the optimization process can create unnecessary compromise of proton plan qualities, especially for those complexly shaped skull-base meningioma cases with critical organs in proximity. We showed that as the probability of the large shifts is small, these worst-case scenarios have limited contributions to the deviations from the base plan dose. When considering the statistical average of all the individual setup uncertainty scenarios, both SFUD and MFO plans showed much better dosimetric index and plan qualities than the

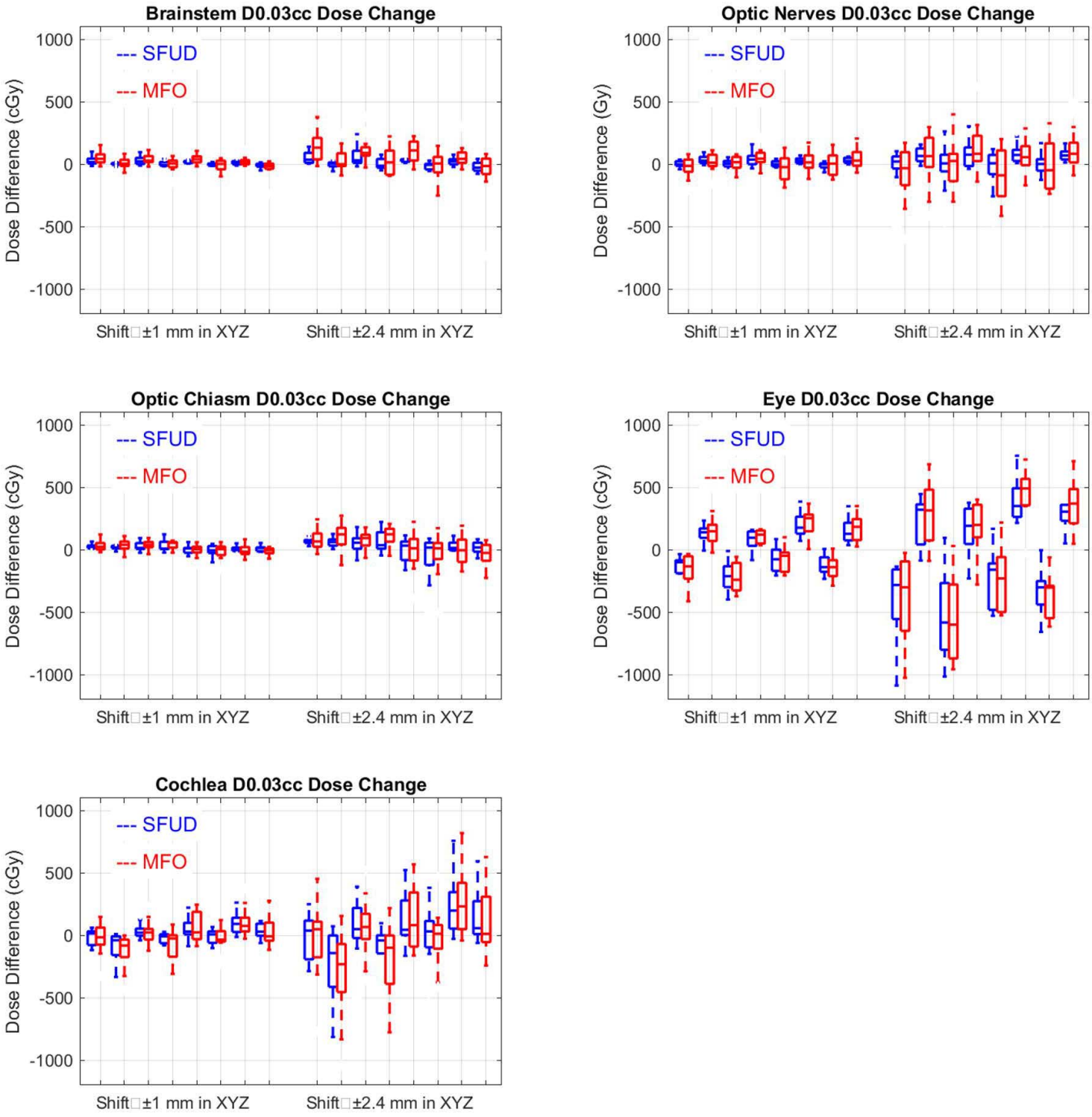

Figure 4. The variations in the OAR dose for all 14 patients due to ±1 mm and ±2.4 mm shifts in X, Y, Z directions from the SFUD and MFO base plans. Each box plot represents the dosimetric index distribution of the patients at the setup uncertainty scenarios of (1.0, 1.0, 1.0), (–1.0, 1.0, 1.0), (1.0, –1.0, 1.0), (–1.0, –1.0, 1.0), (1.0, 1.0, –1.0), (–1.0, 1.0, –1.0), (1.0, –1.0, –1.0), and (–1.0, –1.0, –1.0) mm; and (2.4, 2.4, 2.4), (–2.4, 2.4, 2.4), (2.4, –2.4, 2.4), (–2.4, –2.4, 2.4), (2.4, 2.4, –2.4), (–2.4, 2.4, –2.4), (2.4, –2.4, –2.4), and (–2.4, –2.4, –2.4) mm (from left to right). Abbreviations: MFO, multifield optimization; OAR, organ at risk; SFUD, single-field uniform dose.

Table 4. Statistics of the dosimetric changes in the weighted SFUD and MFO plan sums from the base plans across 14 patients.

Change in	Mean	Std	25%	50%	75%	Min	Max
SFUD							
CTV coverage D99%	1	34	−11	4	21	−86	55
CTV coverage D95%	−1	11	−3	1	6	−34	9
Body D0.03cc	−35	27	−51	−32	−16	−94	3
Brainstem D0.03cc	−11	15	−17	−7	−3	−38	12
Optic nerve D0.03cc	6	18	−1	10	16	−40	39
Optic chiasm D0.03cc	−2	22	−19	2	10	−48	43
Eye D0.03cc	−22	12	−30	−18	−14	−38	−13
Cochlea D0.03cc	5	26	−13	4	18	−25	53
MFO							
CTV coverage D99%	7	18	−4	11	19	−37	34
CTV coverage D95%	5	14	−1	4	11	−23	32
Body D0.03cc	−40	24	−55	−38	−22	−87	3
Brainstem D0.03cc	−15	16	−23	−12	−6	−46	7
Optic nerve D0.03cc	0	20	−9	1	11	−56	30
Optic chiasm D0.03cc	−5	23	−19	3	11	−59	23
Eye D0.03cc	−32	18	−49	−30	−15	−51	−12
Cochlea D0.03cc	−10	25	−27	−8	7	−49	22

Abbreviations: SFUD, single-field uniform dose; MFO, multifield optimization; Std, standard deviation; CTV, clinical target volume; OAR, organ at risk.

Note: The mean, standard deviation, the 25th, 50th, and 75th percentiles, and range of the changes in CTV coverage, body max, and OAR dosimetric index are listed. Values are in cGy.

individual plans. Therefore, we suggest that a probabilistic dose uncertainty model be considered by TPS vendors to build in the future a robust beam optimization module. In the clinic, several TPS systems such as Eclipse and Raystation (RaySearch Laboratories, Stockholm, Sweden) provide a scripting function that can access and modify the treatment plans [26] as well as assess the plan qualities [27]. The scripting application can be used to establish a workflow that can apply the setup shifts to the base plan, recalculate and generate the probability-weighted plan sum, and assess the plan sum quality. This effort would enable more realistic plan evaluations in the clinic, based on the probability of the setup scenarios.

The probability model in this study used the brain setup data from various photon studies. While 6DoF couch for photon treatment is being used more extensively [28], proton systems are generally equipped with 6DoF couches, which can have better positioning of the patient. kV imaging is a standard IGRT method in proton radiation therapy. CBCT in proton radiation therapy is also getting more popular [29]. It would be beneficial to obtain the setup uncertainties for the brain proton radiation therapy treatments. All the efforts in reducing the setup uncertainties will contribute to smaller dose variations from the base plans and result in more consistent proton radiation therapy delivery.

In our study, the range uncertainties due to the calculation algorithm and CT HU (Hounsfield unit) conversion were not included. Our TPS is set up to convert from CT HU values to relative proton-stopping power (RSP) at each CT voxel, based on the HU-RSP calibration curve [30]. A typical uncertainty in the range was estimated to be 3.5% of the range in the body tissue [31], although other range uncertainty values were also proposed [32]. The dosimetric effects from voxel-based HU conversion uncertainties for these PBS plans and the combined effects from the setup and range uncertainties for these skull-base meningioma cases are worth further investigation.

Conclusion

In this study, we analyzed the proton dose impact on the target and critical organs for skull-base meningioma patients with SFUD and MFO planning techniques. From the published IGRT setup uncertainties in the brain treatments, we constructed a bimodal Gaussian distribution model to evaluate plan qualities under various setup scenarios. We demonstrated that in single fraction, large dose deviations in target coverage and organ dose exist. The brainstem, optic nerves, and optic chiasm will have an increase of maximum dose $>$500 cGy at a setup error of 2.4 mm. The probability of such scenario is small. In the most probable 1-mm setup error, the dosimetric impact of these critical organs is $<$260 cGy. Compared with MFO, the proton SFUD planning technique is recommended as it shows more robust target coverage and brainstem dose against setup uncertainties.

When performing a probability-weighted cumulative plan, the dosimetric parameters had <100 cGy impact for all 14 patients studied. The probability-weighted cumulative plan is a closer reflection of the treatment dose that patients would receive rather than a worst-case scenario. The variations in dose coverage due to setup uncertainties in this study could assist in treatment assessment in skull-base meningioma proton radiation therapy. We recommend further development of a robust optimization process using a probability-based setup uncertainty model.

ADDITIONAL INFORMATION AND DECLARATIONS

Conflicts of Interest: Lei Dong, PhD, is an Associate Editor of the *International Journal of Particle Therapy*. The authors have no additional conflicts of interest to disclose.
Funding: The authors have no funding to disclose.
Ethical Approval: All patient data have been collected under internal review board–approved protocol.

References

1. Wiemels J, Wrensch M, Claus EB. Epidemiology and etiology of meningioma. *J Neurooncol*. 2010;99:307–14.
2. Glaholm J, Bloom HJG, Crow JH. The role of radiotherapy in the management of intracranial meningiomas: the Royal Marsden Hospital experience with 186 patients. *Int J Radiat Oncol Biol Phys*. 1990;18:755–61.
3. Wilson CB. Meningiomas: genetics, malignancy, and the role of radiation in induction and treatment: The Richard C. Schneider Lecture. *J Neurosurg*. 1994;81:666–75.
4. Carella RJ, Ransohoff J, Newall J. Role of radiation therapy in the management of meningioma. *Neurosurgery*. 1982;10: 332–9.
5. Milosevic MF, Frost PJ, Laperriere NJ, Wong CS, Simpson WJ. Radiotherapy for atypical or malignant intracranial meningioma. *Int J Radiat Oncol Biol Phys*. 1996;34:817–22.
6. Pirzkall A, Lohr F, Höss A, Wannenmacher M, Debus J, Carol M. Comparison of intensity-modulated radiotherapy with conventional conformal radiotherapy for complex-shaped tumors. *Int J Radiat Oncol Biol Phys*. 2000;48:1371–80.
7. Milker-Zabel S, Zabel-du Bois A, Huber P, Schlegel W, Debus J. Intensity-modulated radiotherapy for complex-shaped meningioma of the skull base: long-term experience of a single institution. *Int J Radiat Oncol Biol Phys*. 2007;68:858–63.
8. Pirzkall A, Debus J, Haering P, Rhein B, Grosser K-H, Höss A, Wannenmacher M. Intensity modulated radiotherapy (IMRT) for recurrent, residual, or untreated skull-base meningiomas: preliminary clinical experience. *Int J Radiat Oncol Biol Phys*. 2003;55:362–72.
9. Baumert BG, Norton IA, Davis JB. Intensity-modulated stereotactic radiotherapy vs. stereotactic conformal radiotherapy for the treatment of meningioma located predominantly in the skull base. *Int J Radiat Oncol Biol Phys*. 2003;57:580–92.
10. Ding D, Starke RM, Hantzmon J, Yen C-P, Williams BJ, Sheehan JP. The role of radiosurgery in the management of WHO Grade II and III intracranial meningiomas. *Neurosurg Focus*. 2013;35:E16.
11. Stafford SL, Pollock BE, Foote RL, Link MJ, Gorman DA, Schomberg PJ, Leavitt JA. Meningioma radiosurgery: tumor control, outcomes, and complications among 190 consecutive patients. *Neurosurgery*. 2001;49:1029–38.
12. Vernimmen FJ, Harris JK, Wilson JA, Melvill R, Smit BJ, Slabbert JP. Stereotactic proton beam therapy of skull base meningiomas. *Int J Radiat Oncol Biol Phys*. 2001;49:99–105.
13. Hug EB, DeVries A, Thornton AF, Munzenrider JE, Pardo FS, Hedley-Whyte ET, Bussiere MR, Ojemann R. Management of atypical and malignant meningiomas: role of high-dose, 3D-conformal radiation therapy. *J Neurooncol*. 2000;48:151–60.
14. Gudjonsson O, Blomquist E, Nyberg G, Pellettieri L, Montelius A, Grusell E, Dahlgren C, Isacsson U, Lilja A, Glimelius B. Stereotactic irradiation of skull base meningiomas with high energy protons. *Acta Neurochir (Wien)*. 1999;141:933–40.
15. Noël G, Habrand J-L, Mammar H, Haie-Meder C, Pontvert D, Dederke S, Régis Ferrand R, Beaudré A, Gaboriaud G, Boisserie G, Mazeron JJ. Highly conformal therapy using proton component in the management of meningiomas. *Strahlenther Onkol*. 2002;178:480–5.
16. Madani I, Lomax AJ, Albertini F, Trnková P, Weber DC. Dose-painting intensity-modulated proton therapy for intermediate- and high-risk meningioma. *Radiat Oncol*. 2015;10:72.

17. Weber DC, Schneider R, Goitein G, Koch T, Ares C, Geismar JH, Schertler A, Bolsi A, Hug EB. Spot scanning-based proton therapy for intracranial meningioma: long-term results from the Paul Scherrer Institute. *Int J Radiat Oncol Biol Phys*. 2012;83:865–71.
18. Weber DC, Lomax AJ, Peter Rutz H, Stadelmann O, Egger E, Timmermann B, Pedroni ES, Verwey J, Miralbell R, Goitein G, Swiss Proton Users Group. Spot-scanning proton radiation therapy for recurrent, residual or untreated intracranial meningiomas. *Radiother Oncol*. 2004;71:251–8.
19. Shields LB, Coons JM, Dedich C, Ragains M, Scalf K, Vitaz TW, Spalding AC. Improvement of therapeutic index for brain tumors with daily image guidance. *Radiat Oncol*. 2013;8:283.
20. Zou W, Dong L, Kevin Teo B-K. current state of image guidance in radiation oncology: implications for PTV margin expansion and adaptive therapy. *Semin Radiat Oncol*. 2018;28:238–47.
21. Oh SA, Yea JW, Kang MK, Park JW, Kim SK. Analysis of the setup uncertainty and margin of the Daily ExacTrac 6D Image Guide System for patients with brain tumors. *PLoS One*. 2016;11:e0151709. doi:10.1371/journal.pone.0151709.
22. The Royal College of Radiologists, Institue of Physics and Engineering in Medicine, Society and College of Radiographers. *On Target: Ensuring Geometric Accuracy in Radiotherapy*. London: The Royal College of Radiologists; 2008.
23. Cubillos Mesías M, Boda-Heggemann J, Thoelking J, Lohr F, Wenz F, Wertz H. Quantification and assessment of interfraction setup errors based on cone beam CT and determination of safety margins for radiotherapy. *PLoS One*. 2016; 11:e0150326. doi:10.1371/journal.pone.0150326.
24. Tryggestad E, Christian M, Ford E, Kut C, Le Y, Sanguineti G, Song DY, Kleinberg L. Inter- and intrafraction patient positioning uncertainties for intracranial radiotherapy: a study of four frameless, thermoplastic mask-based immobilization strategies using daily cone-beam CT. *Int J Radiat Oncol Biol Phys*. 2011;80:281–90.
25. Infusino E, Trodella L, Ramella S, D'Angelillo RM, Greco C, Iurato A, Trodella LE, Nacca A, Cornacchione P, Mameli A. Estimation of patient setup uncertainty using BrainLAB Exatrac X-Ray 6D system in image-guided radiotherapy. *J Appl Clin Med Phys*. 2015;16:99–107.
26. Thomas DH, Miller B, Rabinovitch R, Milgrom S, Kavanagh B, Diot Q, Miften M, Schubert LK. Integration of automation into an existing clinical workflow to improve efficiency and reduce errors in the manual treatment planning process for total body irradiation (TBI). *J Appl Clin Med Phys*. 2020;21:100–6.
27. Liu S, Bush KK, Bertini J, Fu Y, Lewis JM, Pham DJ, Pham DJ, Yang Y, Niedermayr TR, Skinner L, Xing L, Beadle BM, Hsu A, Kovalchuk N. Optimizing efficiency and safety in external beam radiotherapy using automated plan check (APC) tool and six sigma methodology. *J Appl Clin Med Phys*. 2019;20:56–64.
28. Mancosu P, Reggiori G, Gaudino A, Lobefalo F, Paganini L, Palumbo V, Stravato A, Tomatis S, Scorsetti M. Are pitch and roll compensations required in all pathologies: a data analysis of 2945 fractions. *Br J Radiol*. 2015;88:20150468.
29. Landry G, Nijhuis R, Dedes G, Handrack J, Thieke C, Janssens G, Orban de Xivry J, Reiner M, Kamp F, Wilkens JJ, Paganelli C, Riboldi R, Baroni G, Ganswindt U, Belka C, Parodi K. Investigating CT to CBCT image registration for head and neck proton therapy as a tool for daily dose recalculation: CT to CBCT dir for H&N particle therapy. *Med Phys*. 2015; 42:1354–66.
30. Schneider U, Pedroni E, Lomax A. The calibration of CT Hounsfield units for radiotherapy treatment planning. *Phys Med Biol*. 1996;41:111–24.
31. Moyers MF, Miller DW, Bush DA, Slater JD. Methodologies and tools for proton beam design for lung tumors. *Int J Radiat Oncol Biol Phys*. 2001;49:1429–38.
32. Zheng Y, Kang Y, Zeidan O, Schreuder N. An end-to-end assessment of range uncertainty in proton therapy using animal tissues. *Phys Med Biol*. 2016;61:8010–24.